Introduction to the theory of hadronic collisions, and the physics of the LHC
(part II)

CERN Winter School on Supergravity, Strings, and Gauge Theory 2011

Jan 24- 28 2011

Michelangelo L. Mangano

TH Unit, Physics Department, CERN

michelangelo.mangano@cern.ch

Evolution of hadronic final states

Asymptotic freedom implies that at E_{CM} >> 1 GeV

$\sigma(e^+ e^- \to \text{hadrons})$ ⟷ $\sigma(e^+ e^- \to \text{quarks/gluons})$

At the Leading Order (LO) in PT:

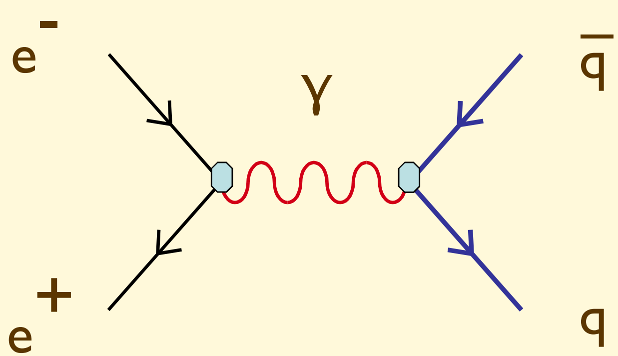

$$\sigma_0(e^+e^- \to q\bar{q}) = \frac{4\pi\alpha^2}{9s} N_c \sum_{f=u,d,\ldots} e^2_{q_f}$$

$$\frac{\sigma_0(e^+e^- \to q\bar{q})}{\sigma_0(e^+e^- \to \mu^+\mu^-)} = N_c \sum_{f=u,d,\ldots} e^2_{q_f}$$

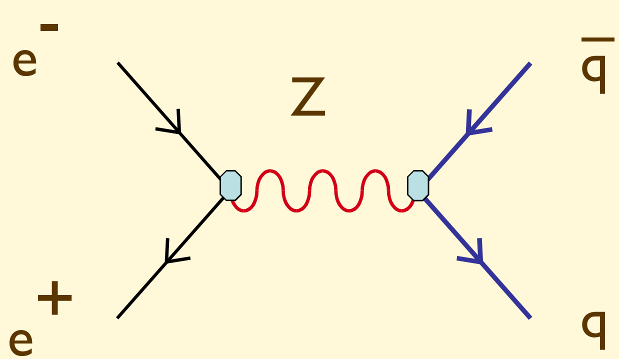

$$\frac{\sigma_0(e^+e^- \to Z \to q\bar{q})}{\sigma_0(e^+e^- \to Z \to \mu^+\mu^-)} = N_c \frac{\sum_{f=u,d,\ldots}\left(v^2_{q_f} + a^2_{q_f}\right)}{\left(v^2_\mu + a^2_\mu\right)}$$

Adding higher-order perturbative terms:

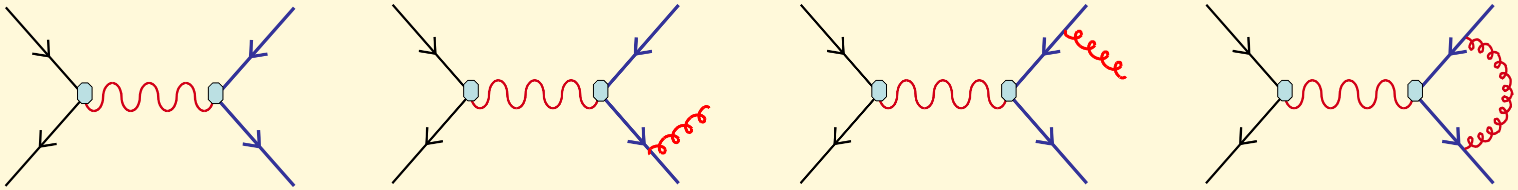

+ ≥2-gluon emissions

$$\sigma_1(e^+e^- \to q\bar{q}(g)) = \sigma_0(e^+e^- \to q\bar{q}) \left(1 + \frac{\alpha_s(E_{CM})}{\pi} + O(\alpha_s^2)\right)$$

O(3%) at M_Z

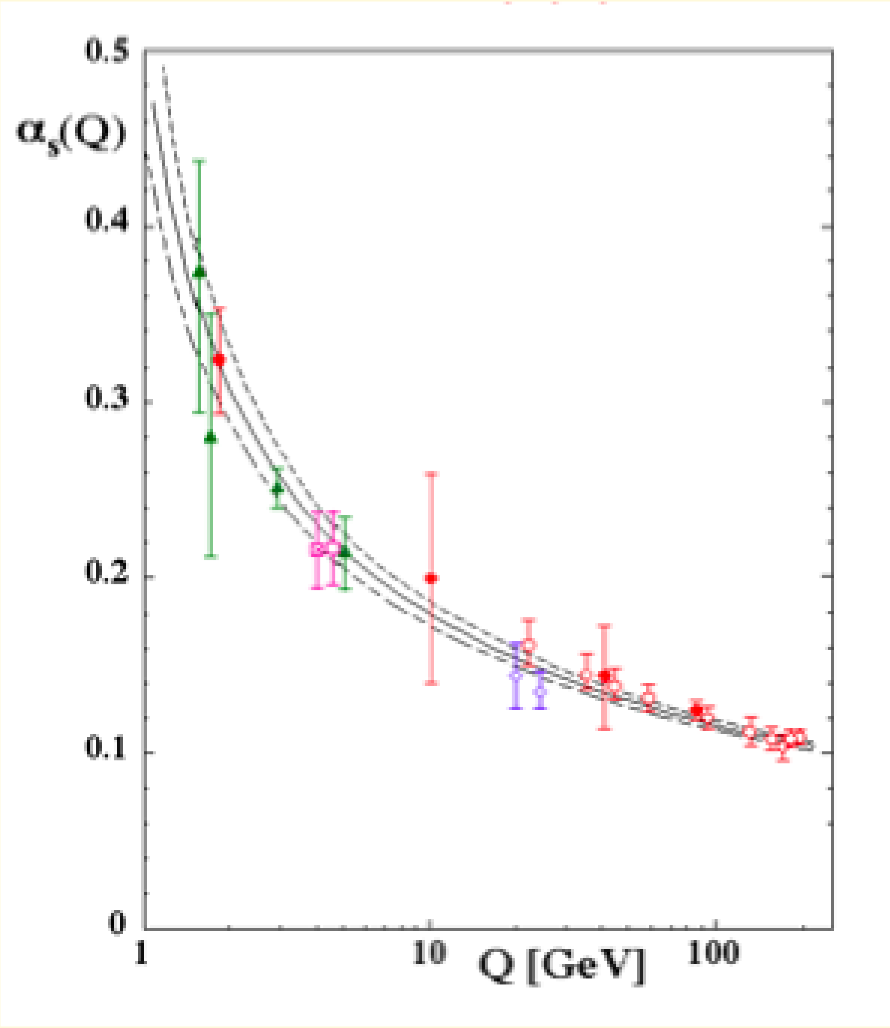

Excellent agreement with data,
provided N_c=3
Extraction of αs consistent with the Q evolution predicted by QCD

Experimentally, the final states contain a large number of particles, not the 2 or 3 which apparently saturate the perturbative cross-section.

Experimental multiplicity distribution

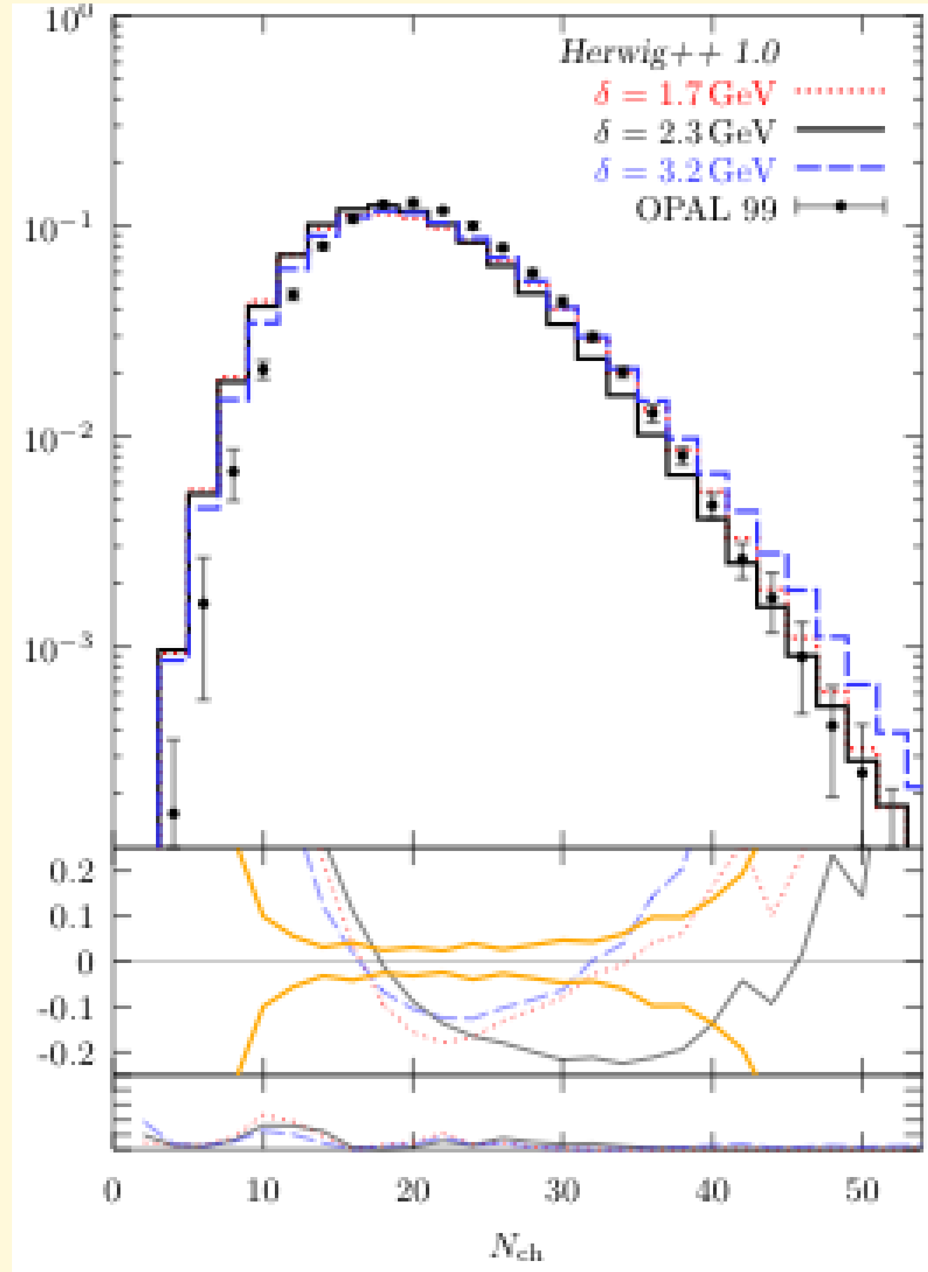

$<n_{charged}> = 20.9$

Isn't this bizarre?

Look more closely at the structure of these events:

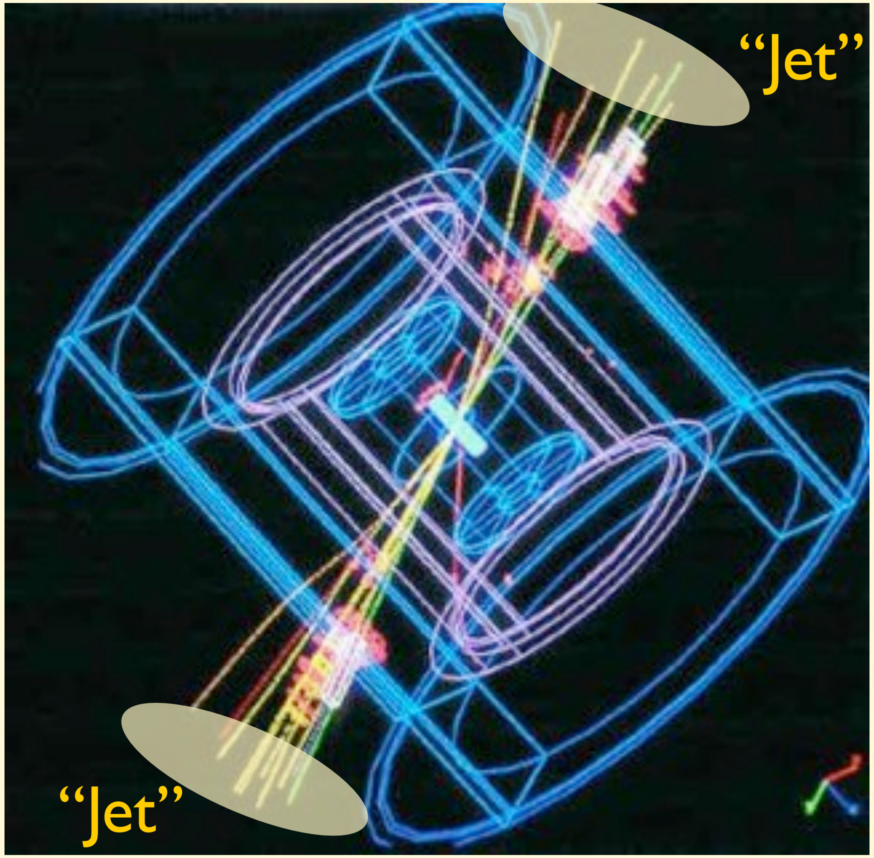

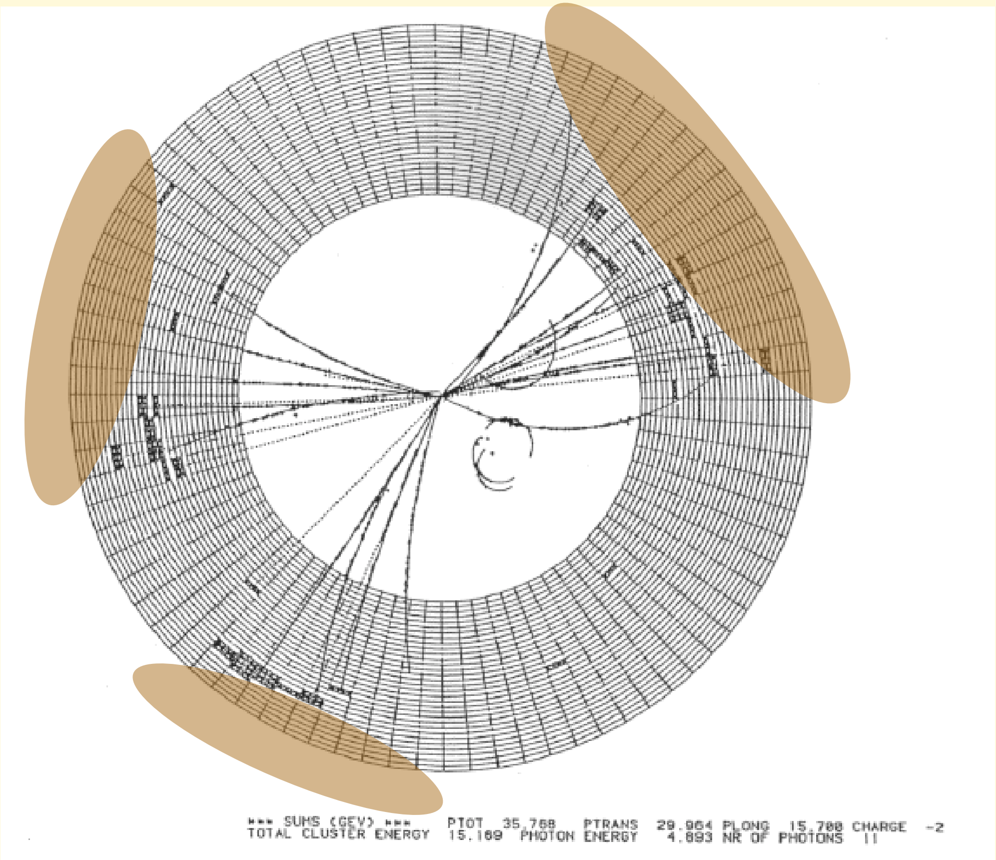

$e^+ e^- \to qq$ ⇨ $e^+ e^- \to$ 2 jets

$e^+ e^- \to qqg$ ⇨ $e^+ e^- \to$ 3 jets

The puzzle appears to be solved by associating partons to collimated "**jets**" of hadrons

Soft gluon emission

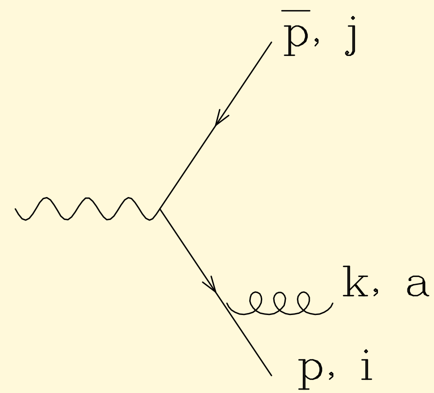

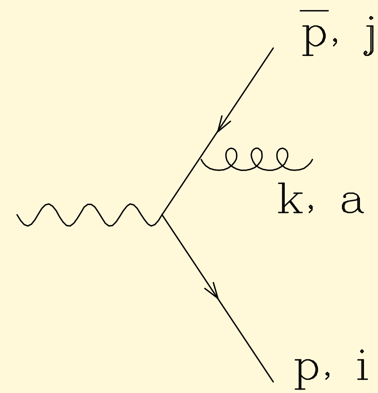

$$
\begin{aligned}
A &= \bar{u}(p)\epsilon(k)(ig)\,\frac{-i}{\not{p}+\not{k}}\,\Gamma^\mu\, v(\bar{p})\ \lambda^a_{ij} + \bar{u}(p)\,\Gamma^\mu\,\frac{i}{\not{\bar{p}}+\not{k}}\,(ig)\epsilon(k)\,v(\bar{p})\ \lambda^a_{ij} \\
&= \left[\frac{g}{2p\cdot k}\,\bar{u}(p)\epsilon(k)\,(\not{p}+\not{k})\Gamma^\mu\, v(\bar{p}) - \frac{g}{2\bar{p}\cdot k}\,\bar{u}(p)\,\Gamma^\mu\,(\not{\bar{p}}+\not{k})\epsilon(k)\,v(\bar{p})\right]\lambda^a_{ij}
\end{aligned}
$$

$p \cdot k = p_0\, k_0\, (1-\cos\theta) \Rightarrow$ singularities for collinear ($\cos\theta \to 1$) or soft ($k_0 \to 0$) emission

Collinear emission does not alter the global structure of the final state, since its preserves its "pencil-like-ness". **Soft emission** at large angle, however, could spoil the structure, and leads to strong interferences between emissions from different legs. So soft emission needs to be studied in more detail.

In the soft ($k_0 \to 0$) limit the amplitude simplifies and factorizes as follows:

$$
A_{soft} = g\lambda^a_{ij}\left(\frac{p\cdot\varepsilon}{p\cdot k} - \frac{\bar{p}\cdot\varepsilon}{\bar{p}\cdot k}\right) A_{Born}
$$

Factorization: it is the expression of the independence of long-wavelength (soft) emission on the nature of the hard (short-distance) process.

Another simple derivation of soft-gluon emission rules

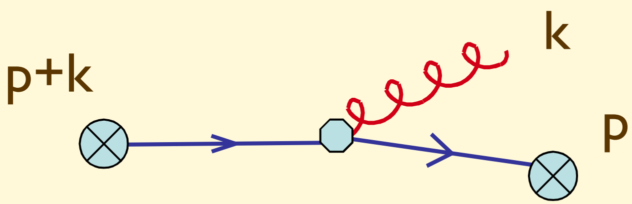

charge current of a free fermion

$$\bar{\psi}(p)\,\gamma_\mu\,\psi(p+k)\,\varepsilon^\mu(k) \;\xrightarrow{k\to 0}\; \bar{\psi}(p)\,\gamma_\mu\,\psi(p)\,\varepsilon^\mu(k) \;=\; 2p\cdot\varepsilon$$

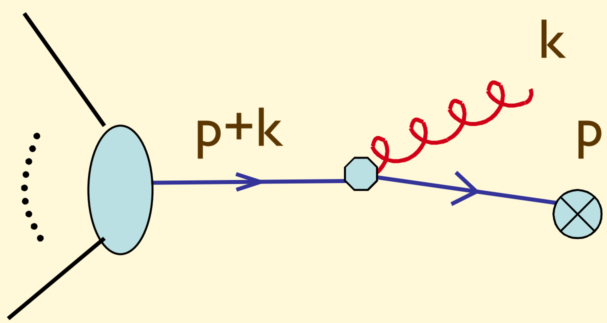

$$\frac{1}{\not{p}+\not{k}}\gamma_\mu\,\psi(p)\,\varepsilon^\mu(k) \;\xrightarrow{k\to 0}$$

$$\frac{1}{2p\cdot k}\,\not{p}\gamma_\mu\,\psi(p)\varepsilon^\mu(k) \;=\; \frac{p\cdot\varepsilon}{p\cdot k}\psi(p)$$

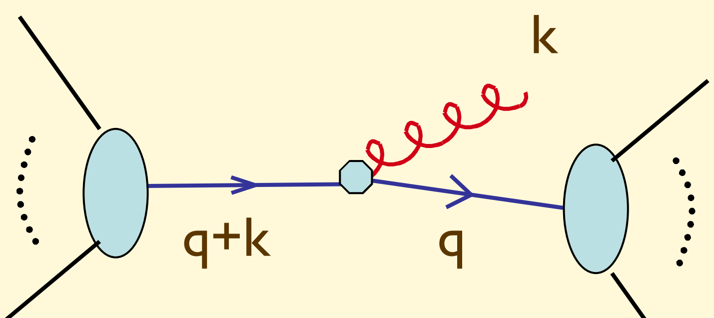

$$\frac{1}{\not{q}+\not{k}}\gamma_\mu\,\frac{1}{\not{q}}\,\varepsilon^\mu(k) \;\xrightarrow{q^2\neq 0,\; k\to 0}\; \frac{1}{q^2}\,\not{q}\gamma_\mu\,\not{q}\,\frac{1}{q^2}\varepsilon^\mu(k)$$

$q^2\neq 0$

=> finite

Similar, but more structured, result in the case of a fully coloured process:

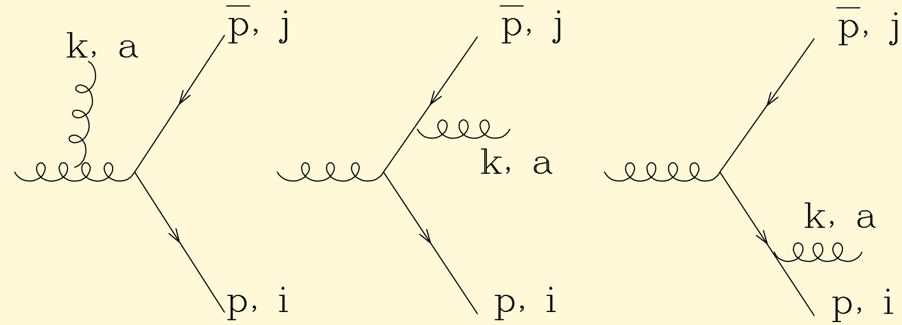

$$A_{soft} = g\,(\lambda^a\lambda^b)_{ij}\left[\frac{Q\varepsilon}{Qk} - \frac{\bar{p}\varepsilon}{\bar{p}k}\right] + g\,(\lambda^b\lambda^a)_{ij}\left[\frac{p\varepsilon}{pk} - \frac{Q\varepsilon}{Qk}\right]$$

The four terms correspond to the two possible ways colour can flow, and to the two possible emissions for each colour flow:

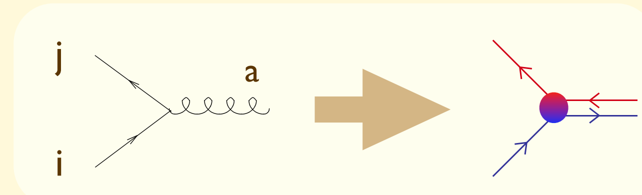

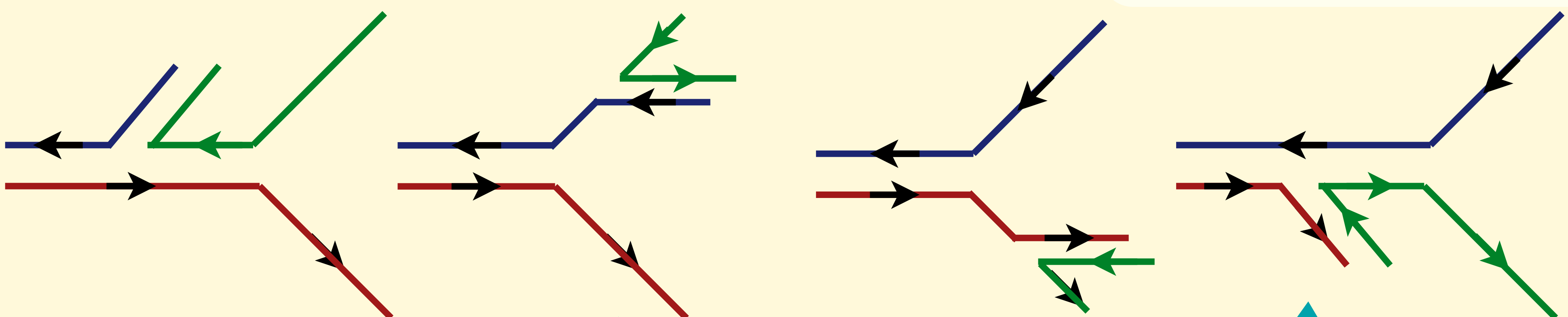

$$A_{soft} = g\,(\lambda^a\lambda^b)_{ij}\left[\frac{Q\varepsilon}{Qk} - \frac{\bar{p}\varepsilon}{\bar{p}k}\right] + g\,(\lambda^b\lambda^a)_{ij}\left[\frac{p\varepsilon}{pk} - \frac{Q\varepsilon}{Qk}\right]$$

The interference between the two colour structures

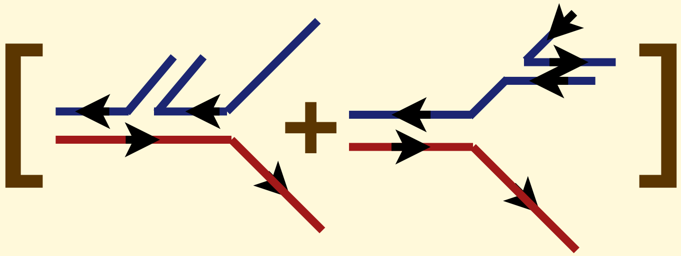 $\propto \; (\lambda^a\lambda^b)_{ij}$ 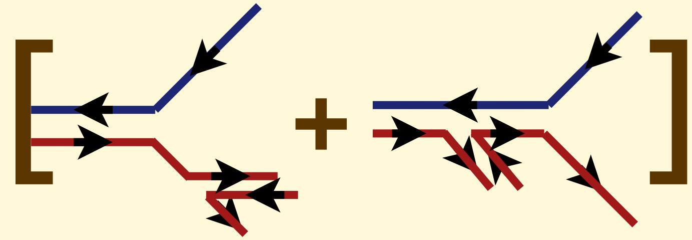 $\propto \; (\lambda^b\lambda^a)_{ij}$

is suppressed by $1/N_c^2$:

$$\sum_{a,b,i,j} |(\lambda^a\lambda^b)_{ij}|^2 = \sum_{a,b} tr\ (\lambda^a\lambda^b\lambda^b\lambda^a) = \frac{N^2-1}{2} C_F = O(N^3)$$

$$\sum_{a,b,i,j} (\lambda^a\lambda^b)_{ij}[(\lambda^b\lambda^a)_{ij}]^* = \sum_{a,b} tr(\lambda^a\lambda^b\lambda^a\lambda^b) = \frac{N^2-1}{2} \underbrace{(C_F - \frac{C_A}{2})}_{-\frac{1}{2N}} = O(N)$$

As a result, the emission of a soft gluon can be described, to the leading order in $1/N_c^2$, as the incoherent sum of the emission from the two colour currents

What about the interference between the two diagrams corresponding to the same colour flow? ➥

Angular ordering

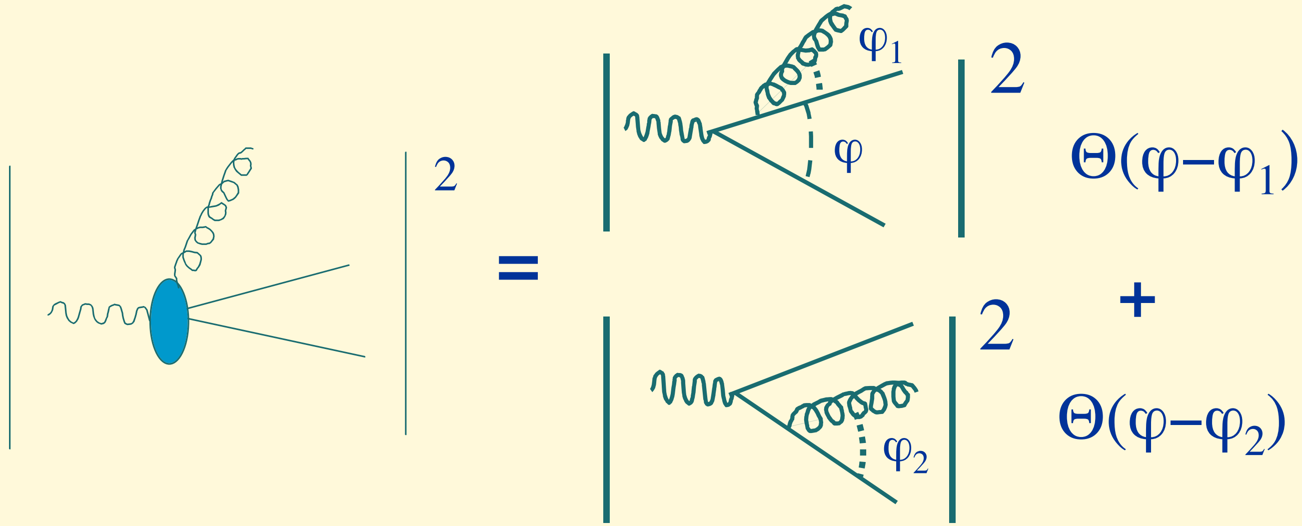

Radiation inside the cones is allowed, and described by the eikonal probability, radiation outside the cones is suppressed and averages to 0 when integrated over the full azimuth

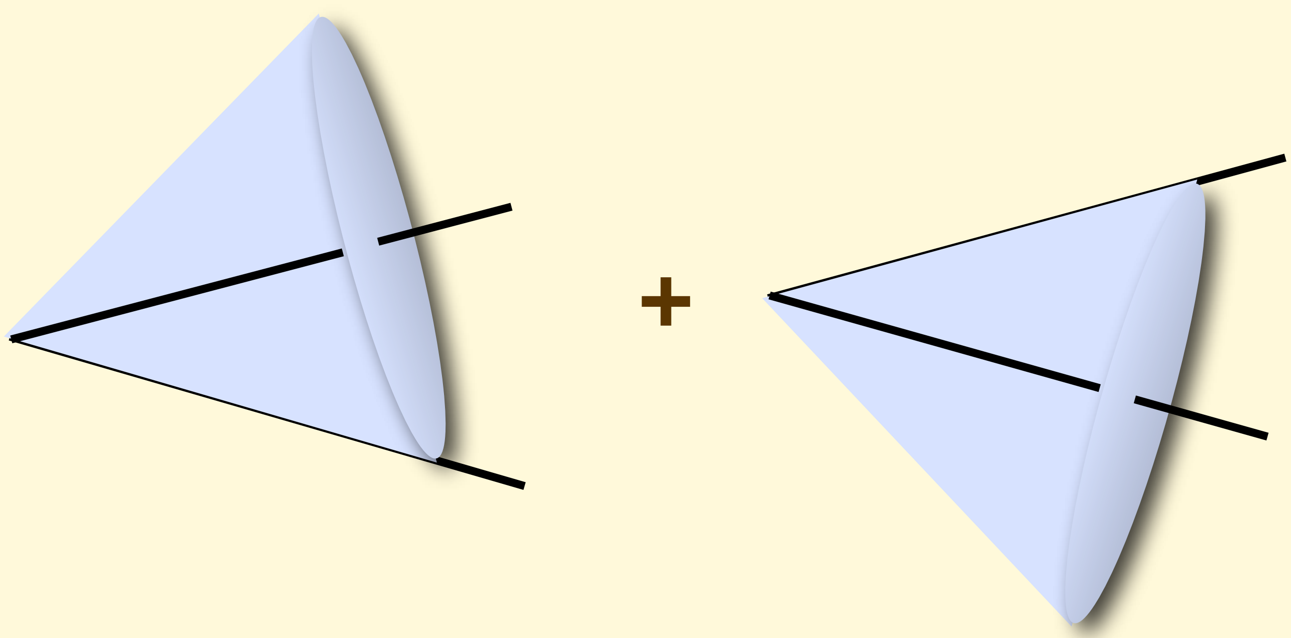

An intuitive explanation of angular ordering

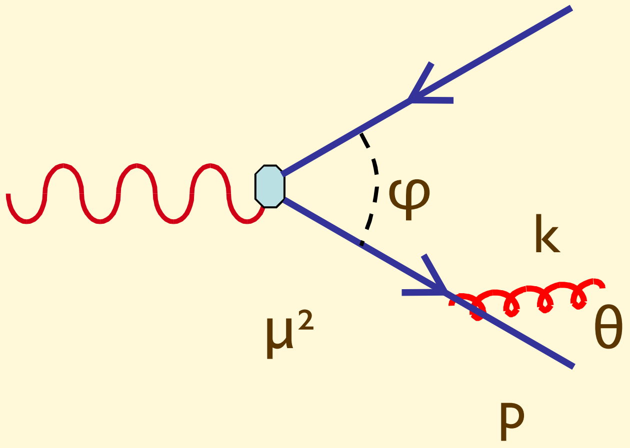

Lifetime of the virtual intermediate state:

$$\tau < \gamma/\mu = E/\mu^2 = 1 / (k_0\theta^2) = 1/(k_\perp\theta)$$

$$\mu^2 = (p+k)^2 = 2E\, k_0\, (1-\cos\theta)$$
$$\sim E\, k_0\, \theta^2 \sim E\, k_\perp\, \theta$$

Distance between q and qbar after τ:

$$d = \varphi\tau = (\varphi/\theta)\ 1/k_\perp$$

If the transverse wavelength of the emitted gluon is longer than the separation between q and qbar, the gluon emission is suppressed, because the q qbar system will appear as colour neutral (=> dipole-like emission, suppressed)

Therefore $d > 1/k_\perp$, which implies $\boxed{\theta < \varphi}$

The formal proof of angular ordering

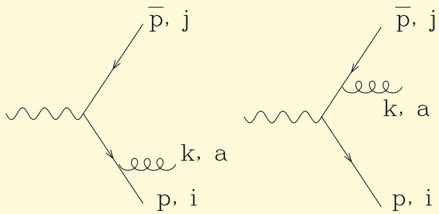

$$d\sigma_g = \sum |A_{soft}|^2 \frac{d^3k}{(2\pi)^3 2k^0} \sum |A_0|^2 \frac{-2p^\mu \bar{p}^\nu}{(pk)(\bar{p}k)} g^2 \sum \varepsilon_\mu \varepsilon_\nu^* \frac{d^3k}{(2\pi)^3 2k^0}$$

$$= d\sigma_0 \frac{\alpha_s C_F}{\pi} \frac{dk^0}{k^0} \frac{d\phi}{2\pi} \frac{1-\cos\theta_{ij}}{(1-\cos\theta_{ik})(1-\cos\theta_{jk})} d\cos\theta$$

You can easily prove that:

$$\frac{1-\cos\theta_{ij}}{(1-\cos\theta_{ik})(1-\cos\theta_{jk})} = \frac{1}{2}\left[\frac{\cos\theta_{jk}-\cos\theta_{ij}}{(1-\cos\theta_{ik})(1-\cos\theta_{jk})} + \frac{1}{1-\cos\theta_{ik}}\right] + \frac{1}{2}[i \leftrightarrow j] \equiv W_{(i)} + W_{(j)}$$

where:

$$W_{(i)} \to finite\ if\ k \parallel j\ (\cos\theta_{jk} \to 1)$$
$$W_{(j)} \to finite\ if\ k \parallel i\ (\cos\theta_{ik} \to 1)$$

The probabilistic interpretation of W(i) and W(j) is a priori spoiled by their non-positivity. However, you can prove that after azimuthal averaging:

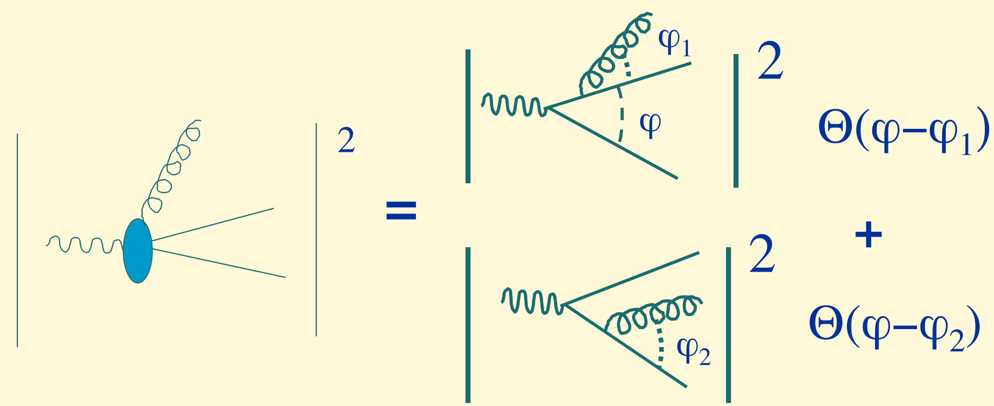

$$\int \frac{d\phi}{2\pi} W_{(i)} = \frac{1}{1-\cos\theta_{ik}} \text{ if } \theta_{ik} < \theta_{ij}\,, \quad 0 \text{ otherwise}$$

$$\int \frac{d\phi}{2\pi} W_{(j)} = \frac{1}{1-\cos\theta_{jk}} \text{ if } \theta_{jk} < \theta_{ij}\,, \quad 0 \text{ otherwise}$$

Further branchings will obey angular ordering relative to the new angles. As a result emission angles get smaller and smaller, squeezing the jet

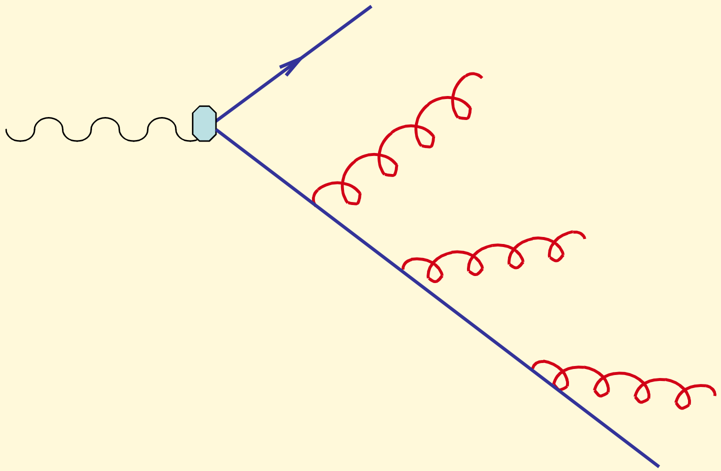

The construction can be iterated to the next emission, with the result that emission angles keep getting smaller and smaller => **jet structure**

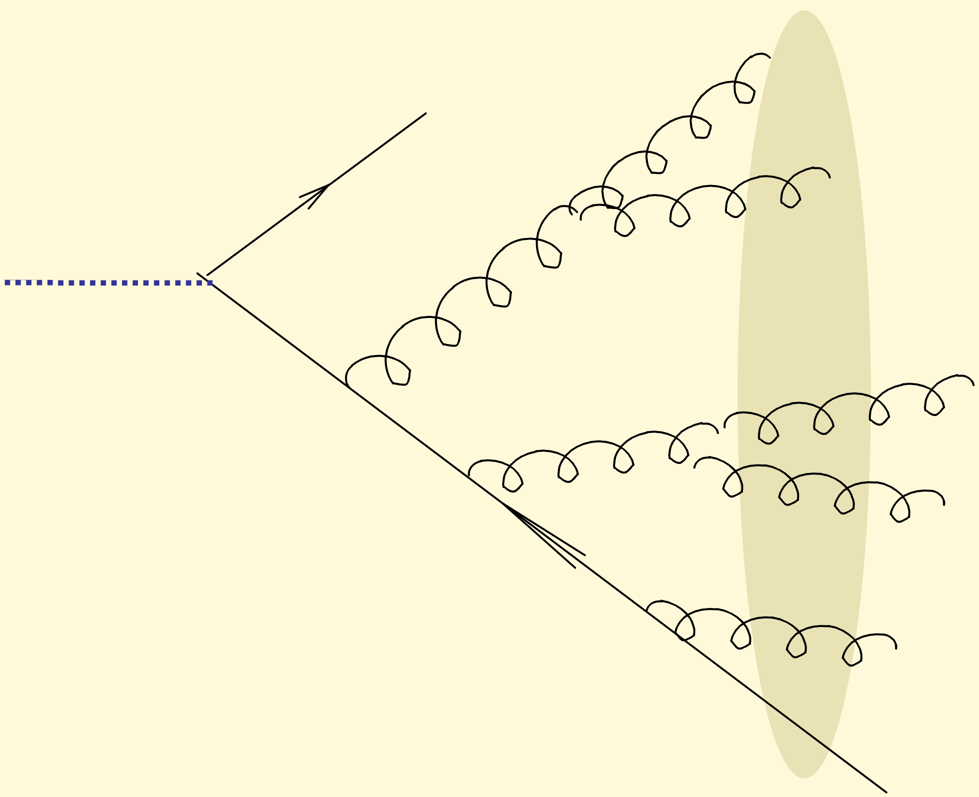

Total colour charge of the system is equal to the quark colour charge. Treating the system as the incoherent superposition of N gluons would lead to artificial growth of gluon multiplicity. Angular ordering enforces coherence, and leads to the proper evolution with energy of particle multiplicities.

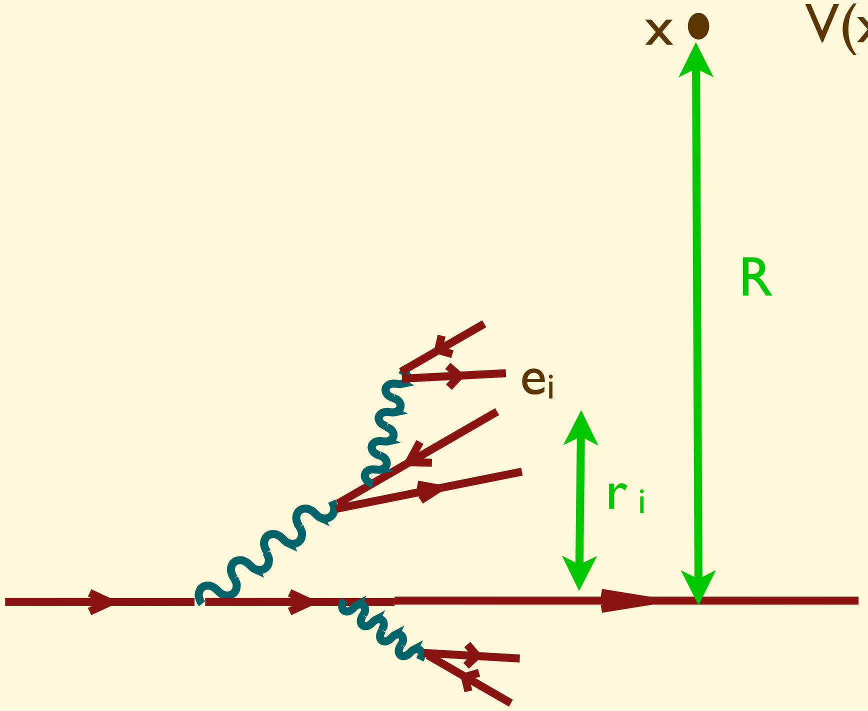

$$V(x) = \frac{e}{R} + \frac{1}{R^2} \left| \sum e_i \mathbf{r}_i \right|$$

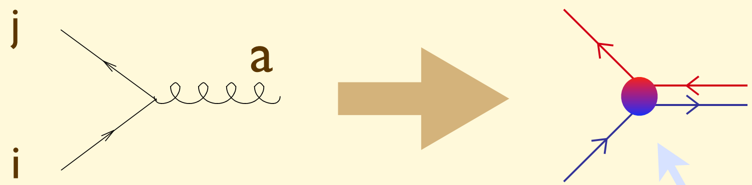

The structure of the perturbative evolution leads naturally to the clustering in phase-space of colour-singlet parton pairs (”preconfinement”). Long-range correlations are strongly suppressed. Hadronization will only act locally, on low-mass colour-singlet clusters.

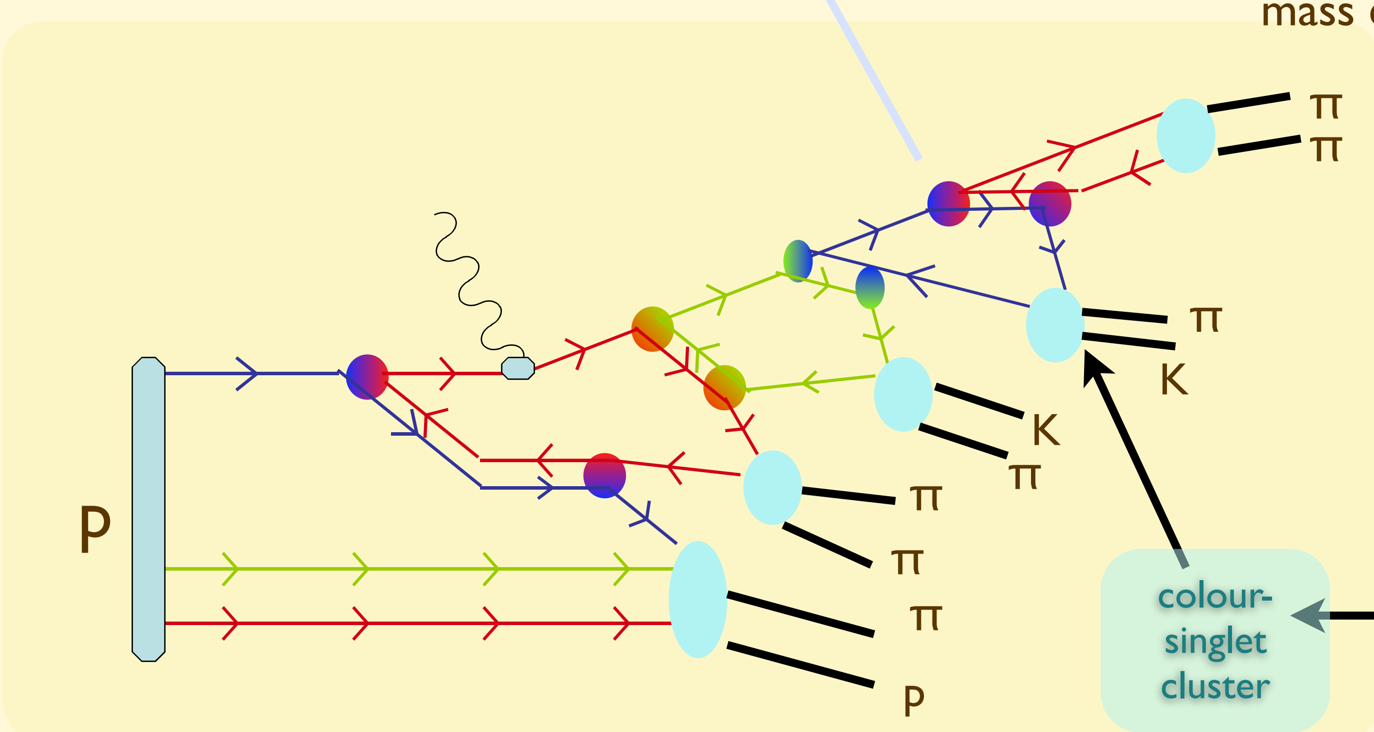

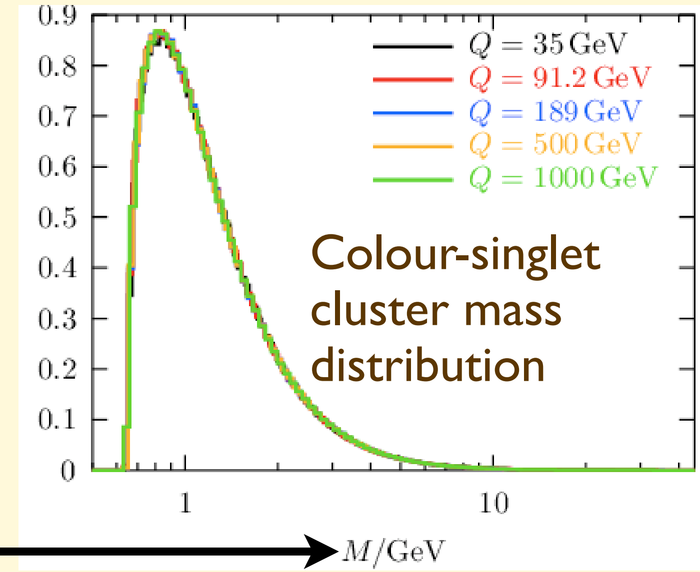

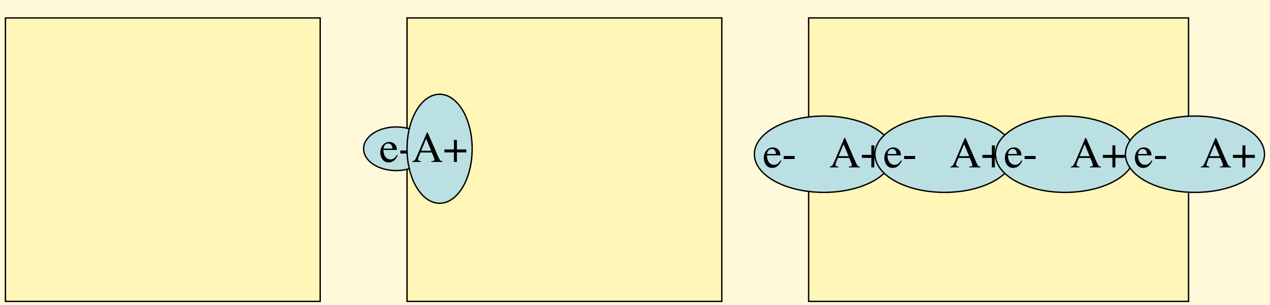

Colour is left “behind” by the struck quark. The first soft gluon emitted at large angle will connect to the beam fragments, ensuring that the beam fragments can recombine to form hadrons, and will allow the struck quark to evolve without having to worry about what happens to the proton fragments.

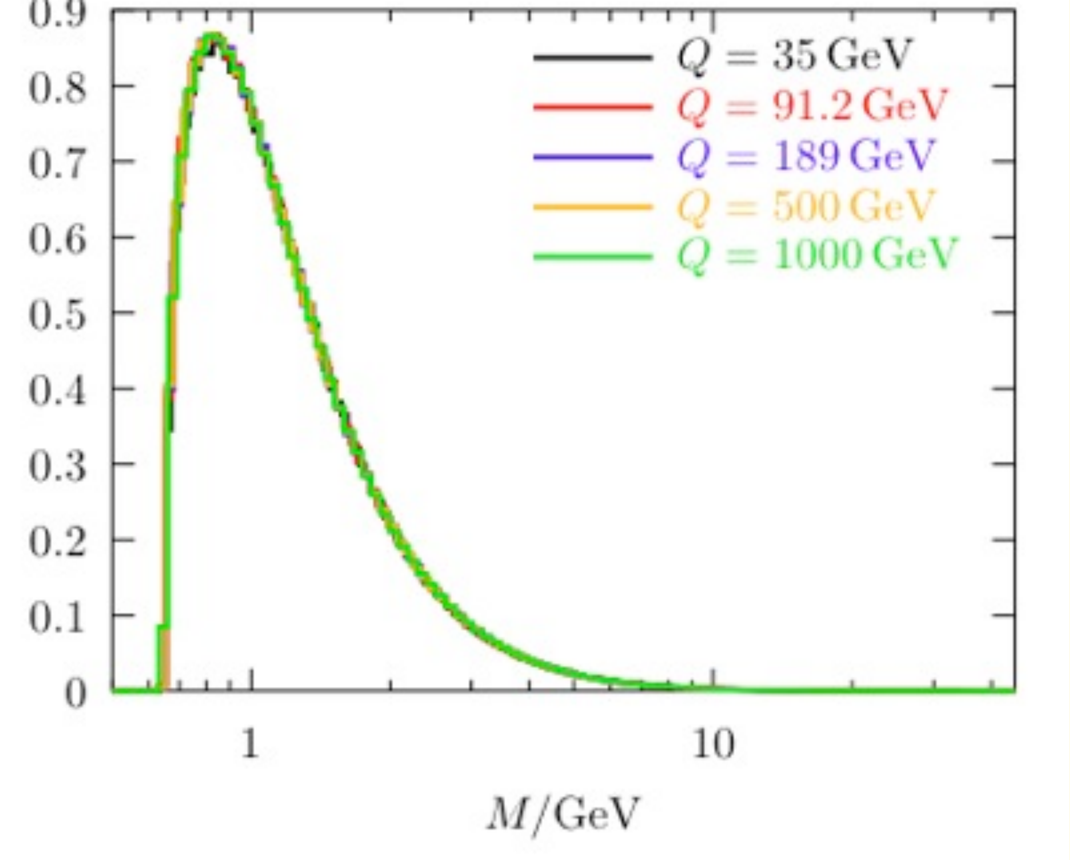

The existence of high-mass clusters, however rare, is unavoidable, due to IR cutoff which leads to a non-zero probability that no emission takes place. This is particularly true for evolution of massive quarks (as in, e.g. Z→bb or cc). Prescriptions have to be defined to deal with the "evolution" of these clusters. **This has an impact on the z→1 behaviour of fragmentation functions.**

Phenomenologically, this leads to uncertainties, for example, in the background rates for H→γγ (jet→γ).

Hadronization

At the end of the perturbative evolution, the final state consists of quarks and gluons, forming, as a result of angular-ordering, low-mass clusters of colour-singlet pairs:

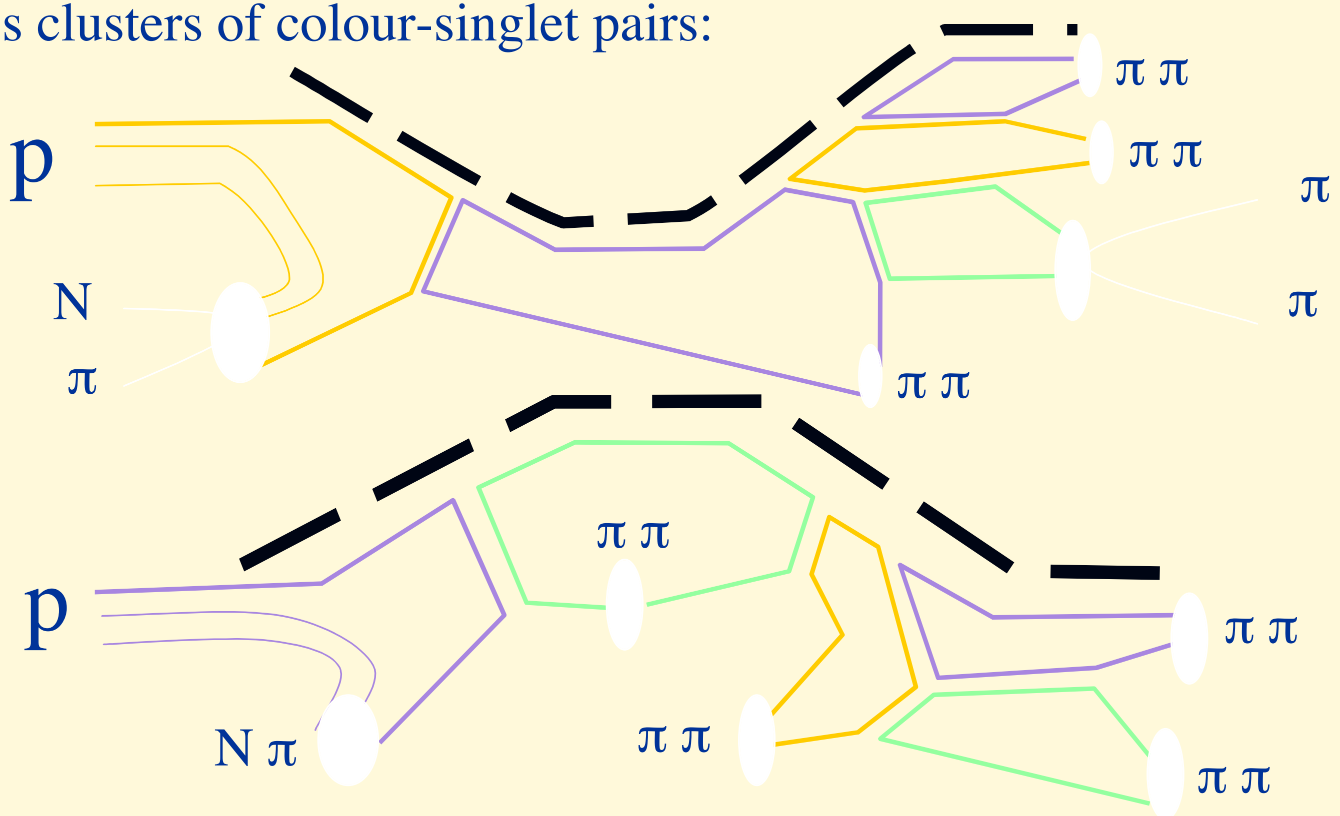

Thanks to the cluster pre-confinement, hadronization is local and independent of the nature of the primary hard process, as well as of the details of how hadronization acts on different clusters. Among other things, one therefore expects:

N(pions) = C N(gluons),
C=constant~2

Example: Drell-Yan processes

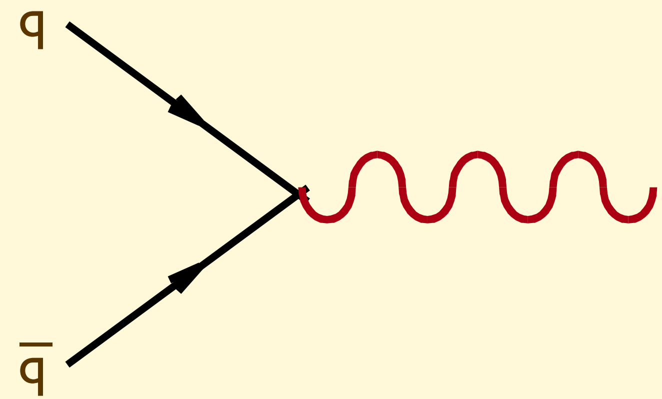

$W \to \ell\nu$

$Z \to \ell^+\ell^-$

Properties/Goals of the measurement:

- Clean final state (no hadrons from the hard process)
- Tests of QCD: $\sigma(W,Z)$ known up to NNLO (2-loops)
- Measure m(W) (→ constrain m(H))
- constrain PDFs (e.g. $f_{up}(x)/f_{down}(x)$)
- search for new gauge bosons: $q\bar{q} \to W', Z'$
- Probe contact interactions: $q\bar{q} \to e^+e^-$

Some useful relations and definitions

Rapidity: $y = \frac{1}{2} \log \frac{E_W + p_W^z}{E_W - p_W^z}$

Pseudorapidity: $\eta = -\log(\tan\frac{\theta}{2})$

where:

$\tan\theta = \frac{p_T}{p^z}$ and $p_T = \sqrt{p_x^2 + p_y^2}$

Exercise: prove that for a massless particle rapidity=pseudorapidity:

Exercise: using $\tau = \frac{\hat{s}}{S} = x_1 x_2$ and

$$\begin{cases} E_W = (x_1 + x_2)\, E_{\text{beam}} \\ p_W^z = (x_1 - x_2)\, E_{\text{beam}} \end{cases} \Rightarrow y = \frac{1}{2} \log \frac{x_1}{x_2}$$

prove the following relations:

$$x_{1,2} = \sqrt{\tau}\, e^{\pm y} \qquad dx_1\, dx_2 = dy\, d\tau$$

$$dy = \frac{dx_1}{x_1} \qquad d\tau\, \delta(\hat{s} - m_W^2) = \frac{1}{S}$$

LO Cross-section calculation

$$\sigma(pp \to W) = \sum_{q,q'} \int dx_1 dx_2\, f_q(x_1,Q)\, f_{\bar{q}'}(x_2,Q)\, \frac{1}{2\hat{s}} \int d[PS]\, \overline{\sum_{spin,col}} |M(q\bar{q}' \to W)|^2$$

where:

$$\overline{\sum_{spin,col}} |M(q\bar{q}' \to W)|^2 = \frac{1}{3}\frac{1}{4} 8 g_W^2 |V_{qq'}|^2 \hat{s} = \frac{2}{3}\frac{G_F m_W^2}{\sqrt{2}} |V_{qq'}|^2 \hat{s}$$

$$d[PS] = \frac{d^3 p_W}{(2\pi)^3 2 p_W^0} (2\pi)^4 \delta^4(P_{in} - p_W)$$

$$= 2\pi\, d^4 p_W\, \delta(p_W^2 - m_W^2)\, \delta^4(P_{in} - p_W) = 2\pi\, \delta(\hat{s} - m_W^2)$$

leading to:

$$\sigma(pp \to W) = \sum_{ij} \frac{\pi A_{ij}}{m_W^2}\, \tau \int_\tau^1 \frac{dx}{x} f_i(x,Q)\, f_j(\frac{\tau}{x},Q) \equiv \sum_{ij} \frac{\pi A_{ij}}{m_W^2}\, \tau L_{ij}(\tau)$$

where:

$$\frac{\pi A_{u\bar{d}}}{m_W^2} = 6.5\text{nb} \quad \text{and} \quad \tau = \frac{m_W^2}{S}$$

Exercise: Study the function $\tau L(\tau)$

Assume, for example, that $f(x) \sim \frac{1}{x^{1+\delta}}\,, \quad 0 < \delta < 1$

Then: $$L(\tau) = \int_\tau^1 \frac{dx}{x} \frac{1}{x^{1+\delta}} \left(\frac{x}{\tau}\right)^{1+\delta} = \frac{1}{\tau^{1+\delta}} \log\left(\frac{1}{\tau}\right)$$

and: $$\sigma_W = \sigma_W^0 \left(\frac{S}{m_W^2}\right)^\delta \log\left(\frac{S}{m_W^2}\right)$$

Therefore the W cross-section grows at least logarithmically with the hadronic CM energy. This is a typical behavior of cross-sections for production of fixed-mass objects in hadronic collisions, contrary to the case of e+e- collisions, where cross-sections tend to decrease with CM energy.

Note also the following relation, which allows the measurement of the total width of the W boson from the determination of the leptonic rates of W and Z bosons,

$$\Gamma_W = \frac{N(e^+e^-)}{N(e^\pm\nu)} \left(\frac{\sigma_{W^\pm}}{\sigma_Z}\right) \left(\frac{\Gamma^W_{e\nu}}{\Gamma^Z_{e^+e^-}}\right) \Gamma_Z$$

LHC data

theory

LEP/SLC

Searching new forces at the LHC: W', Z'

E.g. a W' coupling to R-handed fermions, to reestablish at high energy the R/L symmetry

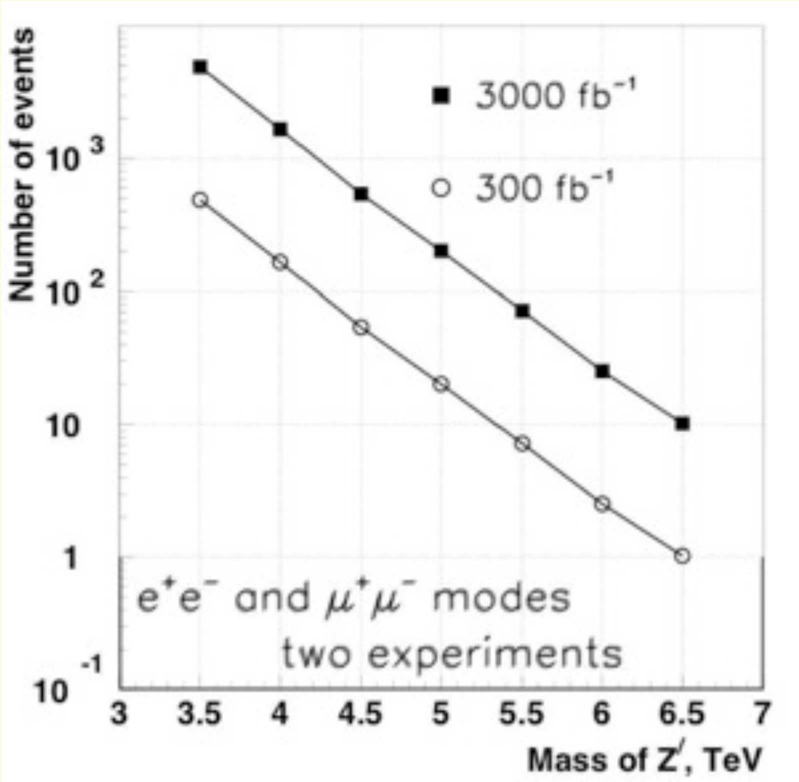

100 fb^{-1} discovery reach up to ~ 5.5 TeV

but ....

Differentiating among different Z' models:

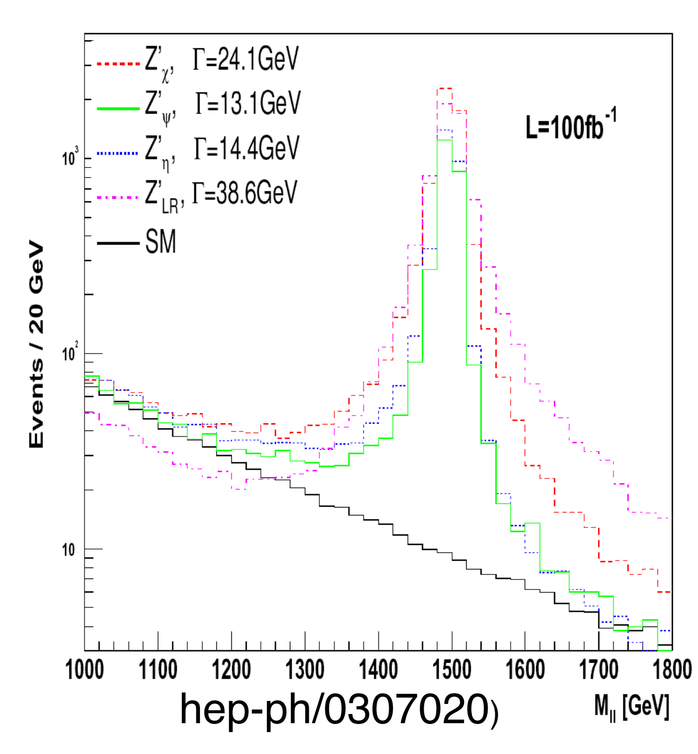

hep-ph/0307020)

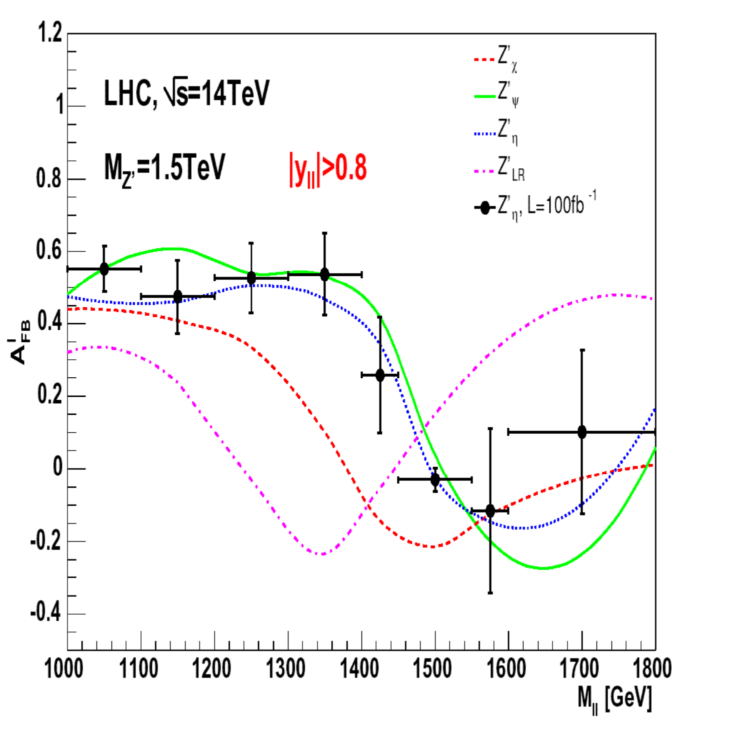

100 fb^{-1} model discrimination up to 2.5 TeV

Jets in hadronic collisions

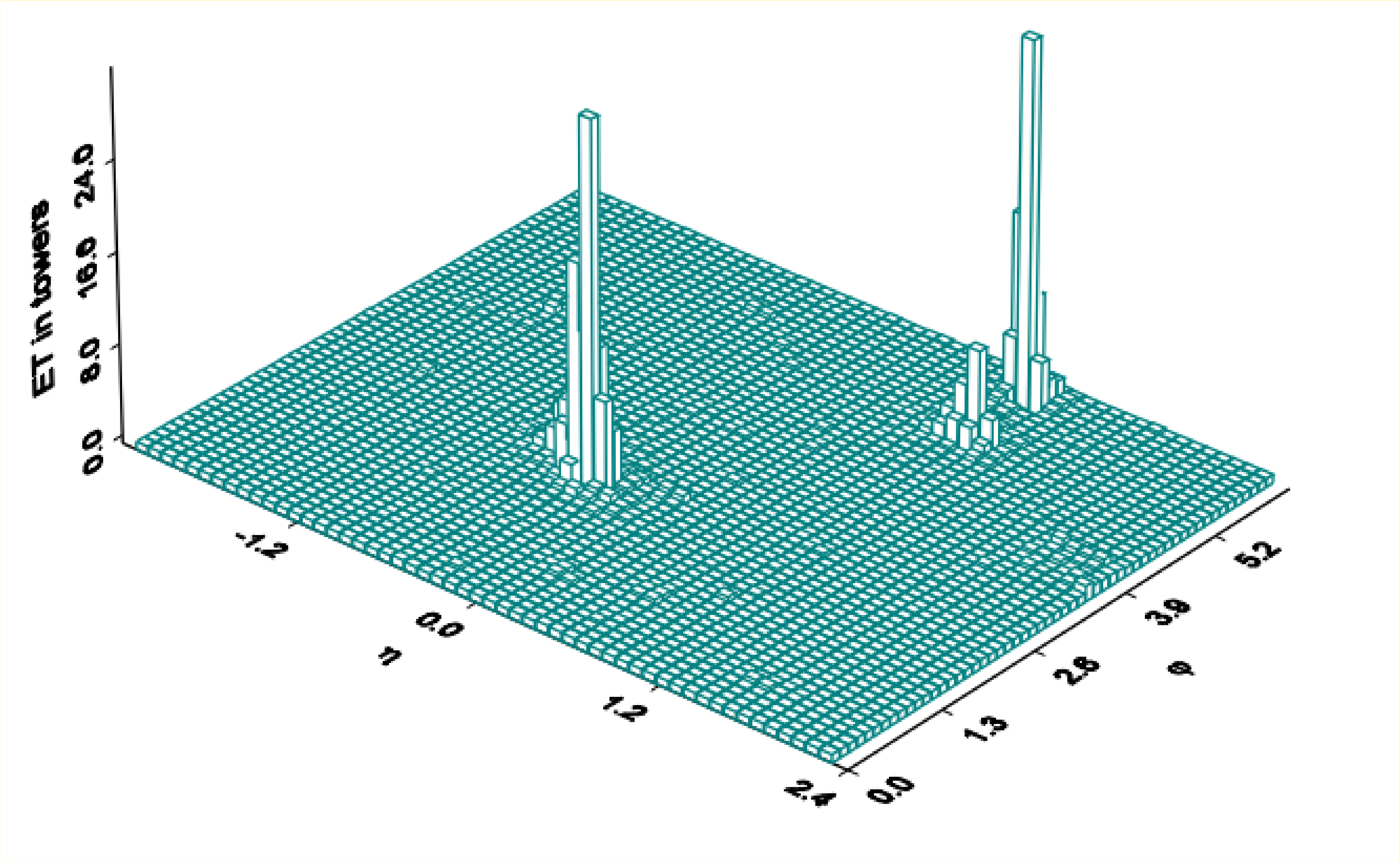

- Inclusive production of jets is the largest component of high-Q phenomena in hadronic collisions
- QCD predictions are known up to NLO accuracy
- Intrinsic theoretical uncertainty (at NLO) is approximately 10%
- Uncertainty due to knowledge of parton densities varies from 5-10% (at low transverse momentum, p_T to 100% (at very high p_T, corresponding to high-x gluons)
- Jet are used as probes of the quark structure (possible substructure implies departures from point-like behaviour of cross-section), or as probes of new particles (peaks in the invariant mass distribution of jet pairs)

$gg \to gg$

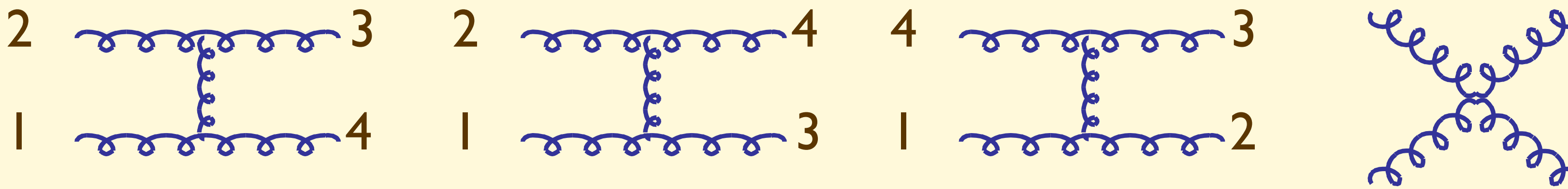

$gg \to q\bar{q}$

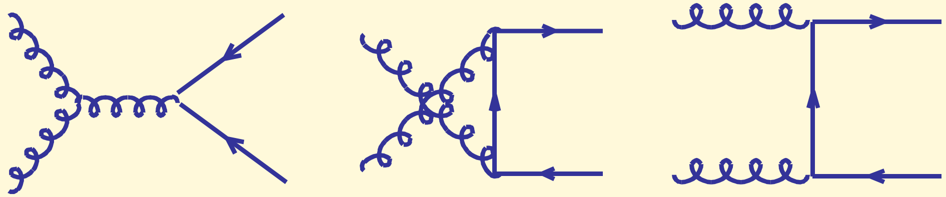

$qg \to qg$

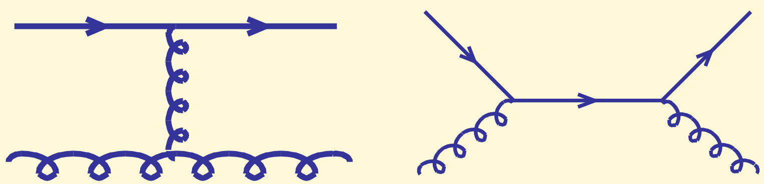

$q\bar{q} \to gg$

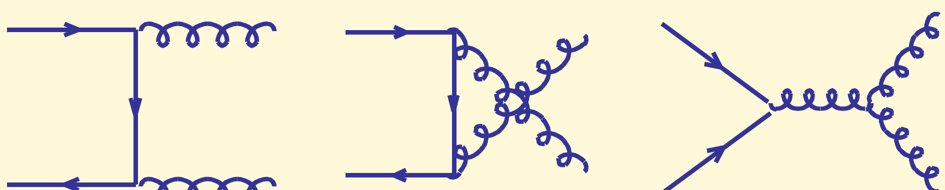

$qq' \to qq'$

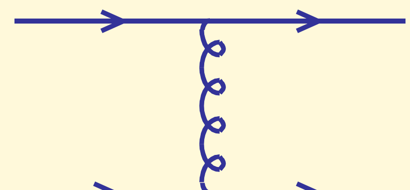

$q\bar{q} \to q\bar{q}$

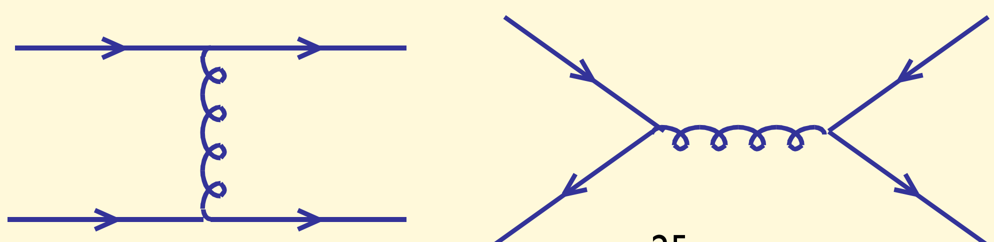

Phase space and cross-section for LO jet production

$$d[PS] = \frac{d^3 p_1}{(2\pi)^2 2p_1^0} \frac{d^3 p_2}{(2\pi)^2 2p_2^0} (2\pi)^4 \delta^4(P_{in} - P_{out})\, dx_1\, dx_2$$

(a) $$\delta(E_{in} - E_{out})\,\delta(P^z_{in} - P^z_{out})\, dx_1\, dx_2 = \frac{1}{2E^2_{beam}}$$

(b) $$\frac{dp^z}{p^0} = dy \equiv d\eta$$

$$\boxed{d[PS] = \frac{1}{4\pi S} p_T\, dp_T\, d\eta_1\, d\eta_2}$$

$$\boxed{\frac{d^3\sigma}{dp_T d\eta_1 d\eta_2} = \frac{p_T}{4\pi S} \sum_{i,j} f_i(x_1)\, f_j(x_2) \frac{1}{2\hat{s}} \overline{\sum_{kl}} |M(ij \to kl)|^2}$$

The measurement of pT and rapidities for a dijet final state uniquely determines the parton momenta x_1 and x_2. Knowledge of the partonic cross-section allows therefore the determination of partonic densities f(x)

Small-angle jet production, a useful approximation for the determination of the matrix elements and of the cross-section

At small scattering angle, $t=(p_1-p_3)^2 \sim (1-\cos\theta) \to 0$

and the $1/t^2$ propagators associated with t-channel gluon exchange dominate the matrix elements for all processes. In this limit it is easy to evaluate the matrix elements. For example:

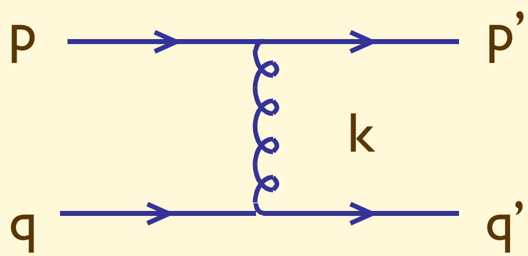

$$\sim (\lambda^a)_{ij}(\lambda^a)_{kl}(2p_\mu)\frac{1}{t}(2q_\mu) = \frac{2s}{t}(\lambda^a)_{ij}(\lambda^a)_{kl}$$

where we used the fact that, for k=p-p'<<p (small angle scattering),

$$\bar{u}(p')\gamma_\mu u(p) \sim \bar{u}(p)\gamma_\mu u(p) = 2p_\mu$$

Using our colour algebra results, we then get: $\overline{\sum_{col,spin}}|M|^2 = \frac{1}{N_c^2}\frac{N_c^2-1}{4}\frac{4s^2}{t^2}$

Noting that the result must be symmetric under s↔u exchange, and setting Nc=3, we finally obtain: $\overline{\sum_{col,spin}}|M|^2 = \frac{4}{9}\frac{s^2+u^2}{t^2}$

which turns out to be the exact result!

Quark-gluon and gluon-gluon scattering

We repeat the exercise in the more complex case of qg scattering, assuming the dominance of the t-channel gluon-exchange diagram:

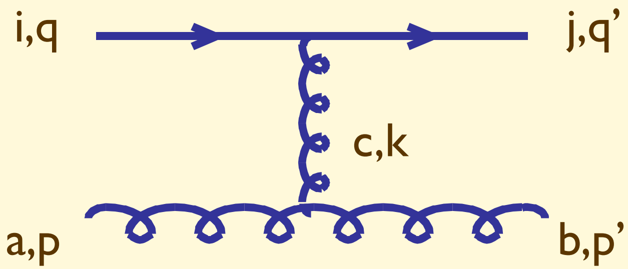

$$\sim f^{abc}\lambda^c_{ij}\, 2p_\mu \frac{1}{t} 2q_\mu = 2\frac{s}{t} f^{abc}\lambda^c_{ij}$$

Using the colour algebra results, and enforcing the s↔u symmetry, we get:

$$\overline{\sum_{col,spin}} |M|^2 = \frac{s^2+u^2}{t^2}$$

which differs by only 20% from the exact result

$$\overline{\sum_{col,spin}} |M|^2 = \frac{s^2+u^2}{t^2} - \frac{4}{9}\frac{s^2+u^2}{us}$$

even in the large-angle region, at 90°

In a similar way we obtain for gg scattering (using the t↔u symmetry):

$$\overline{\sum_{col,spin}} |M(gg \to gg)|^2 = \frac{9}{2}\left(\frac{s^2}{t^2} + \frac{s^2}{u^2}\right)$$

compared to the exact result

$$\overline{\sum_{col,spin}} |M(gg \to gg)|^2 = \frac{9}{2}\left(3 - \frac{ut}{s^2} - \frac{us}{t^2} - \frac{st}{u^2}\right)$$

with a 20% difference at 90°

Note that in the leading 1/t approximation we get the following result:

$$\hat{\sigma}_{gg} : \hat{\sigma}_{qg} : \hat{\sigma}_{qq} = \frac{9}{4} : 1 : \frac{4}{9}$$

where 4/9 = C_F / C_A = [(N^2-1)/2N] / N is the ratio of the squared colour charges of quarks and gluons

and therefore

$$d\sigma_{jet} = \int dx_1 dx_2 \sum_{ij} f_i(x_1) f_j(x_2) d\hat{\sigma}_{ij} = \int dx_1 dx_2 \sum_{ij} F(x_1) F(x_2) d\hat{\sigma}_{gg}$$

where we defined the `effective parton density' F(x):

$$F(x) = g(x) + \frac{4}{9} \sum_i [q_i(x) + \bar{q}_i(x)]$$

As a result jet data cannot be used to extract separately gluon and quark densities. On the other hand, assuming an accurate knowledge of the quark densities (say from HERA), jet data can help in the determination of the gluon density

Process	$\frac{d\hat{\sigma}}{d\Phi_2}$	at 90°
$qq' \to qq'$	$\frac{4}{9}\frac{\hat{s}^2+\hat{u}^2}{\hat{t}^2}$	2.22
$qq \to qq$	$\left[\frac{4}{9}\left(\frac{\hat{s}^2+\hat{u}^2}{\hat{t}^2}+\frac{\hat{s}^2+\hat{t}^2}{\hat{u}^2}\right)-\frac{8}{27}\frac{\hat{s}^2}{\hat{u}\hat{t}}\right]$	3.26
$q\bar{q} \to q'\bar{q}'$	$\frac{4}{9}\frac{\hat{t}^2+\hat{u}^2}{\hat{s}^2}$	0.22
$q\bar{q} \to q\bar{q}$	$\left[\frac{4}{9}\left(\frac{\hat{s}^2+\hat{u}^2}{\hat{t}^2}+\frac{\hat{t}^2+\hat{u}^2}{\hat{s}^2}\right)-\frac{8}{27}\frac{\hat{u}^2}{\hat{s}\hat{t}}\right]$	2.59
$q\bar{q} \to gg$	$\left[\frac{32}{27}\frac{\hat{t}^2+\hat{u}^2}{\hat{t}\hat{u}}-\frac{8}{3}\frac{\hat{t}^2+\hat{u}^2}{\hat{s}^2}\right]$	1.04
$gg \to q\bar{q}$	$\left[\frac{1}{6}\frac{\hat{t}^2+\hat{u}^2}{\hat{t}\hat{u}}-\frac{3}{8}\frac{\hat{t}^2+\hat{u}^2}{\hat{s}^2}\right]$	0.15
$gq \to gq$	$\left[-\frac{4}{9}\frac{\hat{s}^2+\hat{u}^2}{\hat{s}\hat{u}}+\frac{\hat{u}^2+\hat{s}^2}{\hat{t}^2}\right]$	6.11
$gg \to gg$	$\frac{9}{2}\left(3-\frac{\hat{t}\hat{u}}{\hat{s}^2}-\frac{\hat{s}\hat{u}}{\hat{t}^2}-\frac{\hat{s}\hat{t}}{\hat{u}^2}\right)$	30.4

Quark/gluon composition

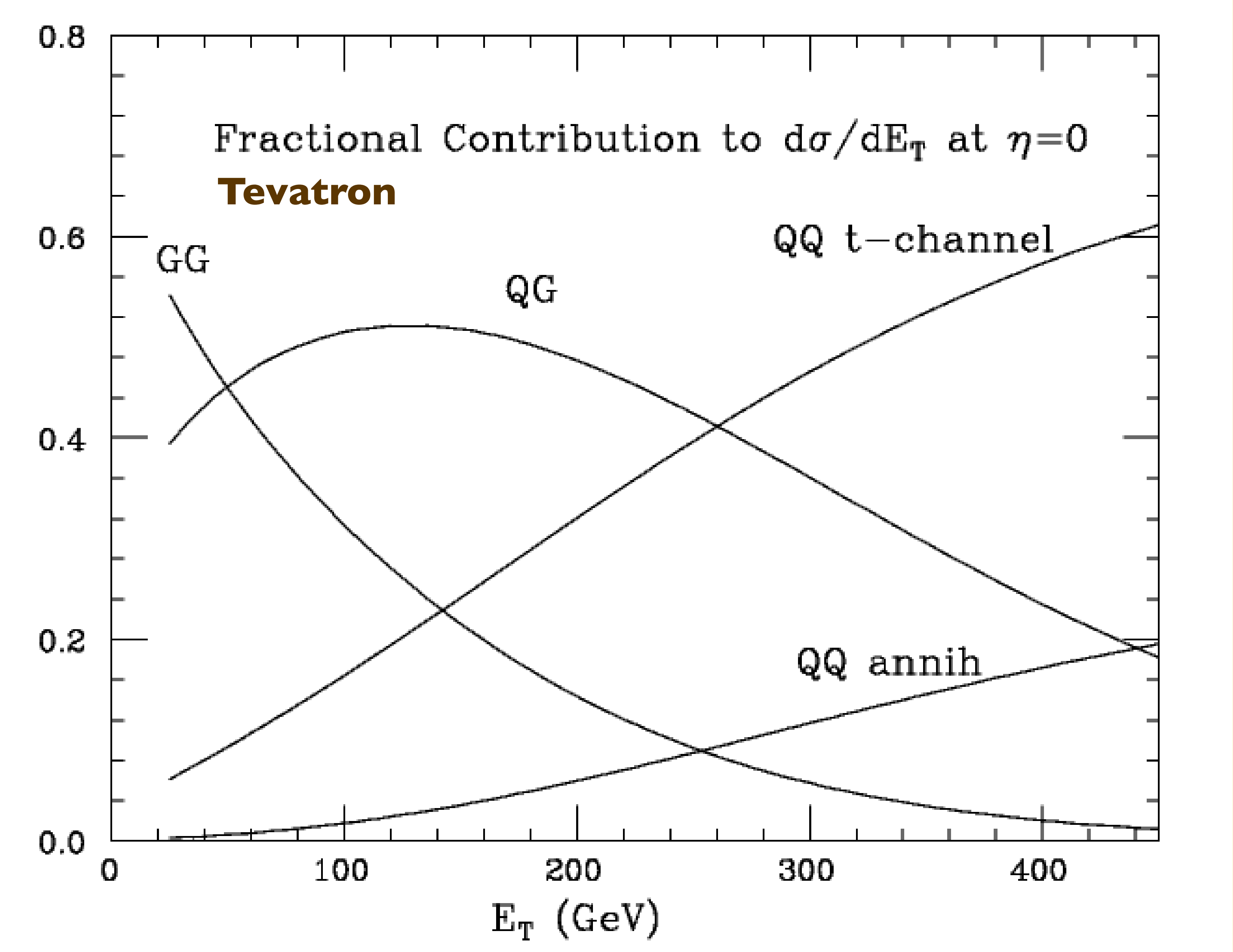

Jet production rates at the LHC, subprocess composition

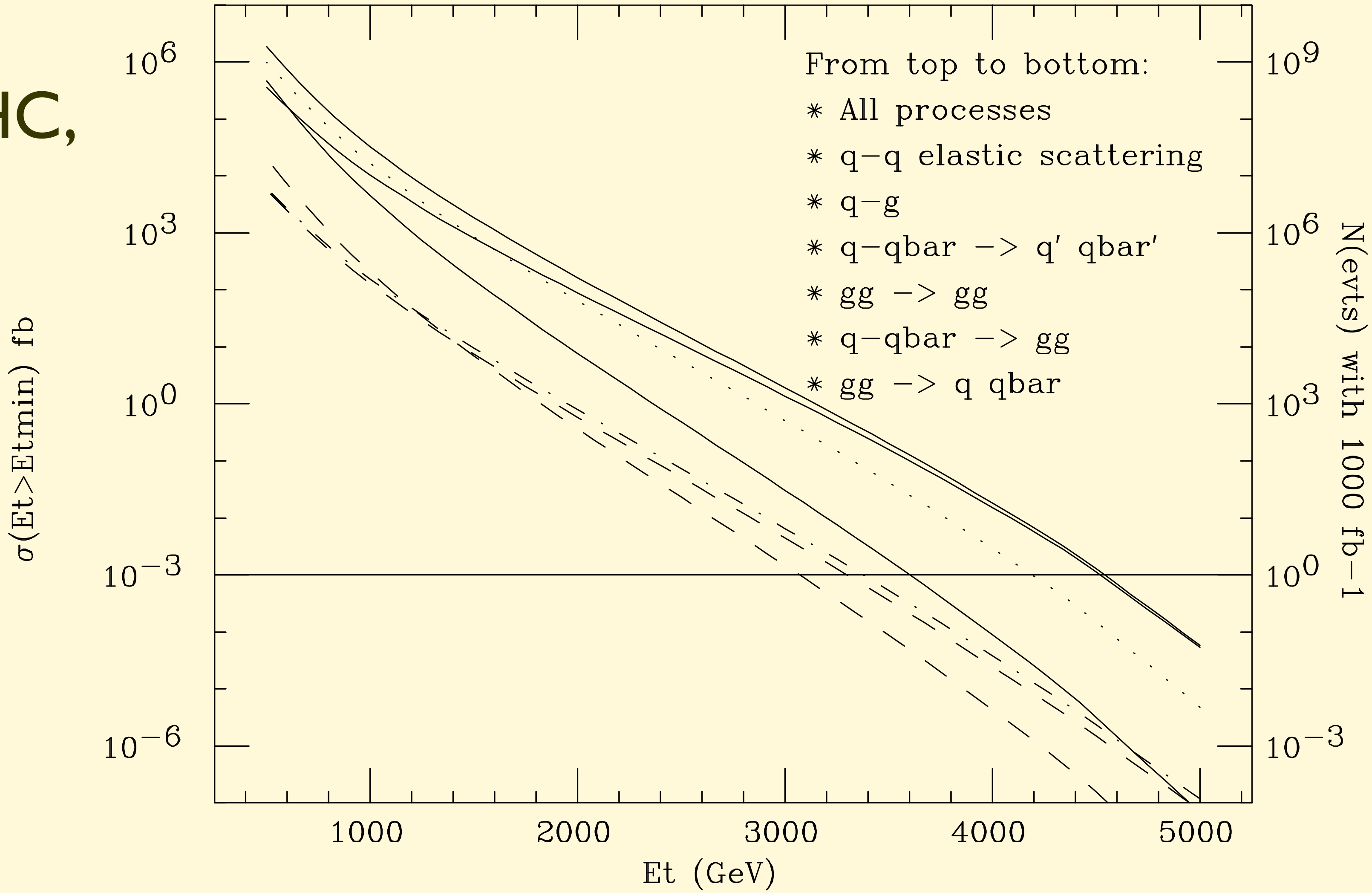

The presence of a quark substructure would manifest itself via contact interactions (as in Fermi's theory of weak interactions). On one side these new interactions would lead to an increase in cross-section, on the other they would affect the jets' angular distributions. In the dijet CMF, QCD implies Rutherford law, and extra point-like interactions can then be isolated using a fit. With the anticipated statistics of 300 fb-1, limits on the scale of the new interactions in excess of 40 TeV should be reached (to increase to 60 TeV with 3000 fb-1)